Synergistic effect of short- and long-read sequencing on functional meta-omics

Valentina Galata[1,#], Susheel Bhanu Busi[1,#], Benoît Josef Kunath[1], Laura de Nies[1], Magdalena Calusinska[2], Rashi Halder[1], Patrick May[1], Paul Wilmes[1], Cédric Christian Laczny[1]*

[1] Luxembourg Centre for Systems Biomedicine, 7, avenue des Hauts-Fourneaux, Esch-sur-Alzette, L-4362, Luxembourg

[2] BioSystems and Bioprocessing Engineering, Luxembourg Institute of Science and Technology, Rue du Brill 41, Belvaux, L-4422, Luxembourg

* Corresponding author

[#] Equal contribution

valentina.galata@uni.lu, susheel.busi@uni.lu, benoit.kunath@uni.lu, laura.denies@uni.lu, magdalena.calusinska@list.lu, rashi.halder@uni.lu, patrick.may@uni.lu, paul.wilmes@uni.lu, cedric.laczny@uni.lu

Abstract

Real-world evaluations of metagenomic reconstructions are challenged by distinguishing reconstruction artefacts from genes and proteins present *in situ*. Here, we evaluate short-read-only, long-read-only, and hybrid assembly approaches on four different metagenomic samples of varying complexity and demonstrate how they affect gene and protein inference which is particularly relevant for downstream functional analyses. For a human gut microbiome sample, we use complementary metatranscriptomic, and metaproteomic data to evaluate the metagenomic data-based protein predictions. Our findings pave the way for critical assessments of metagenomic reconstructions and we propose a reference-independent solution based on the synergistic effects of multi-omic data integration for the *in situ* study of microbiomes using long-read sequencing data.

Keywords

Third-generation sequencing, long reads, Oxford Nanopore Technologies, short reads, hybrid assembly, metagenomics, metatranscriptomics, metaproteomics, functional omics, meta-omics

Background

Third-generation, single-molecule, long-read (LR) sequencing is considered to be the next frontier of genomics [1], especially in the context of studying microbial populations [2,3]. Given the ability to attain read lengths in excess of 10 Kbp [4] and sequence accuracy improvements [5], LR sequencing has been recommended for its ability to resolve GC-rich regions, complex and repetitive loci, and segmental duplications in genomes [4]. However, LR applications to study microbiomes have focused on genome assemblies [6,7], closing a select few bacterial genomes [8], haplotype and strain resolution [9] as well as mock (low diversity) communities [3]. Stewart *et al.*, recently were among the first to demonstrate the utility of using LRs for improving upon existing protein databases owing to a large collection of novel proteins and enzymes identified [10], thereby hinting at the benefits of LR also for functional microbiome studies.

Single base-accuracy of raw LRs remains lower - for now - compared to short-read (SR) methodologies [11]. Several approaches including assembly-based and/or including polishing steps have been developed [11–13] to increase the accuracy. The impact of remnant errors in LR assemblies on gene calling and thereby protein prediction was recently highlighted by Watson *et al*. [14]. Hybrid (HY) assembly methods [15,16] using both SRs and LRs have been proposed to further reduce the error rates compared to LR-only assemblies. While Watson *et al*. [14] showed that insertions/deletions (indels) play a critical role in microbial protein identification, the overall impact of assembly methods on understanding the functional potential of microbial communities is lacking.

Here, we demonstrate that metagenomic assembly methods (SR, LR and HY) not only differ markedly in their overall assembly performance, but also in the inferred functional potential. We reveal the effects of the assembly method on predicted genes and proteins in samples with a low to high diversity, from mock communities to human fecal and rumen metagenomes. We found proteins which are exclusive to respective assemblers and additionally demonstrate using metatranscriptomic and metaproteomic data available for the human fecal sample the synergistic effect on protein verification. Our results indicate that irrespective of sample diversity, the

sequencing and assembly strategies impact downstream analyses and that complementary omics are a key dimension for functional analyses of microbiomes.

Results and Discussion

To understand how sample diversity, assembly quality, and assembly approach are linked, we assembled published metagenomic (metaG) data from a mock community (Zymo), a natural whey starter culture (NWC), a cow rumen sample (Rumen), and a novel metagenomic dataset from a human fecal sample (GDB) which was complemented with metatranscriptomic (metaT) and metaproteomic (metaP) data. The samples' diversity ranged from low (Zymo and NWC) to high (GDB and Rumen). As expected [10], the assembly approach affected strongly the quality of the resulting assembly (Supp. Fig. 1). LR and HY approaches generated fewer contigs with a larger N50 value. However, other assembly metrics, e.g., the total assembly length, varied between the samples and assembly types. The metaG read mapping rate (including multi-mapped reads), as a proxy of data usage, was unaffected by the assembler choice when considering all contigs, though the values for the LR assemblies were a bit lower than for SR or HY assemblies of the high-diversity samples (GDB and Rumen). However, the mapping rates dropped markedly in SR assemblies, especially in NWC and Rumen, when filtering out contigs below 5000bps (Supp. Fig. 2). In GDB, we observed higher metaT read mapping rates in SR and HY assemblies than in LR assemblies. This indicates the complementarity of SR and LR data. The mapping rates decreased considerably in SR assemblies when removing short contigs (Supp. Fig. 3) suggesting the presence of expressed genes located on these contigs. This demonstrates the loss of information when contigs below a certain threshold are removed, which is frequently done in metagenomic studies.

Comparing assemblies pairwise, we observed higher dissimilarities between the LR and SR/HY assemblies than within the latter groups. Additionally, OPERA-MS-based HY assemblies clustered together with the SR assemblies on which they were based (Supp. Fig. 4). To assess functional potential overlap between the different assembly approaches, we studied the proteins found in the individual metagenomes. The overall number and quality of predicted proteins was highly influenced by the assembly approach. In highly diverse metagenomes (GDB and Rumen), the total number of proteins in SR and HY assemblies was higher (by a factor of up to 3.67) than in LR assemblies (Fig 1i). However, throughout all samples, the SR and HY approaches produced more partial proteins (incomplete CDS). We clustered the predicted protein sequences and found a considerable number of proteins exclusive to individual assembly. We also found proteins that

were shared within a subset of the assemblies only. Furthermore, we observed that increased sample diversity resulted in an overall increase in the number of exclusive proteins (Fig 1ii).

As reported previously by Watson *et al.* [14], errors in LR assemblies can have an impact on the predicted proteins. To evaluate how the sample diversity might affect this, we mapped the predicted proteins against the UniProtKB/TrEMBL non-redundant (nr) protein database and computed the query/subject length ratio. In all cases, the density distribution of the ratio values had two peaks (below 0.5 and around 1) though the differences between the assembly methods varied across the samples (Supp. Fig. 5). Considering the above findings and despite multiple rounds of polishing, we cannot disregard the impact of errors in long reads affecting the results. Furthermore, we are aware that the results may also be affected by the sequencing depth and gene prediction methods. One also has to account for the microbial composition per sample, given that a large proportion of proteins from the Rumen sample might not have homologs within the used database.

Due to the differences in annotations, which we found to be exclusive to individual assembly approaches, we subsequently studied the effect of assembler choice on two well defined, functionally relevant classes of genes: ribosomal RNA (rRNA) and antimicrobial resistance (AMR) genes. Overall, the total number of rRNA genes recovered by LR and HY approaches was higher across all samples. Within the archaeal and bacterial domains, LR and HY assemblies led to the prediction of more complete genes compared to SR (Supp. Fig. 6). When analysing AMR proteins and focusing only on “strict” hits (i.e. excluding loose hits flagged as “nudged” by the RGI tool, see Methods), HY assemblers were more adept at identifying these proteins compared to either SR or LR. Moreover, LR assemblies contained more “nudged” hits than SR or HY assemblies, suggesting that error rates or other factors might have affected the reconstruction of some AMR genes (Fig 2i). Interestingly, we did not identify any AMR hits in the NWC metagenome, possibly due to it being a food-grade additive [17]. When comparing the overlap of the Antibiotic Resistance Ontology (ARO) terms covered by “strict” hits, we found that some AROs were only identified in SR and HY assemblies, but not in LR, whereas no AROs were found in LR assemblies only (Fig 2ii).

To validate the exclusive AROs found in SR and HY assemblies, we assessed metaT and metaP coverage of the corresponding genes and proteins in the GDB sample. The genes mapping to the exclusive AROs had an average metaT coverage above 14x in the SR and HY assemblies suggesting that these genes are expressed *in situ*; the few “nudged” hits were below 6x (Supp. Tab. 1). However, we did not identify these genes in the metaP data potentially due to low expression levels, variation in extraction protocols, and/or post-translational modifications

affecting the peptide/proteomic recovery. Though no “strict” hits were found in LR assemblies, some of their “nudged” hits had an average metaT coverage above 10x. To understand why these seemingly expressed genes obtained only a partial hit, we focused on two “nudged” hits assigned to ARO 3004454 (a chloramphenicol acetyltransferase) in the LR assembly constructed with Flye. We found that the corresponding coding sequences (CDSs) were located on the same contig and had an overlap of 29 bps. The sequence alignments showed that the respective genes represent two fragments of the true CDS (corresponding to ARO 3004454) most likely created by an indel which introduced a frameshift and also a premature stop codon. This finding was also supported by the metaT coverage extending beyond the stop codon of the first CDS until the end of the second CDS with a single drop in coverage before the putative indel (Fig 2iii).

To identify high-confidence proteins without the need for a reference, we first considered proteins and protein clusters found in all assemblies which represented 22.97% of the proteins and 8.54% of the protein clusters. These included genes reconstructed by the different and independent assembly approaches, thus lending mutual support. We then used the complementary metaT data and included all additional proteins with an average metaT coverage >= 10x and the corresponding protein clusters. This doubled the number of high-confidence protein clusters (17.63%) and increased the percentage of high-confidence proteins to 30.32%.

Conclusions

We reveal that sample diversity, along with assembly-mediated effects influence prediction of genes and proteins. This causes discrepancies between the assemblies, thereby requiring complementary means to validate these predictions. The observed discrepancies included conserved and also functionally relevant genes (rRNA and antimicrobial resistance genes, respectively), potentially impacting phylogenetic as well as functional studies. To overcome this, we propose a reference-independent approach to identify high-confidence genomic reconstructions by combining metagenomic and metatranscriptomic data. Overall, we show that the sequencing approach and assembly strategy can have a significant impact on the characterization of the microbiome’s functional potential and demonstrate the added value of multi-omic strategies for reconstruction quality evaluation, i.e. going beyond their original purpose, to resolve the functional microbiome.

Methods

Freshly collected human fecal samples from a healthy volunteer (GDB) were immediately flash-frozen in liquid nitrogen and stored at −80 °C; high-molecular weight (HMW) DNA was obtained following the protocol proposed recently [8], with minor modifications; samples were sequenced on Illumina and Oxford Nanopore MinION respectively. Metagenomic sequencing data of three publicly available samples was included: the Zymo mock community (Zymo) [3], a natural whey starter culture (NWC) [17] and a cow rumen (Rumen) [10] dataset. Assemblies were built from short reads (SR), long reads (LR), and short and long reads (HY). The LR and HY assemblies were polished. All assemblies were annotated by predicting rRNA genes and proteins, and matching the latter to the CARD database [18]. For each sample, assemblies were compared, and proteins were clustered. For the GDB sample, metatranscriptomic (metaT) and metaproteomic (metaP) data were additionally used in the downstream analysis. Detailed information on extraction, sequencing and analysis can be found in the Supplementary Information.

Abbreviations

- SR: short reads
- LR: long reads
- HY: hybrid (approach/assembly)
- metaG: metagenomic (data)
- metaT: metatranscriptomic (data)
- metaP: metaproteomic (data)
- AMR: antimicrobial resistance
- rRNA: ribosomal RNA

Declarations

Ethics approval and consent to participate

This study conformed to the Declaration of Helsinki and was approved by the ethics committee of the Physician’s Board Hessen, Germany (FF38/2016).

Consent for publication

All authors acknowledge the content of this manuscript and consent to its publication.

Availability of data and materials

Processed sequencing data of the GDB sample is available under BioProject accession PRJNA723028 (Biosamples: metag_sr: SAMN18797629, metat_sr: SAMN18797630, and metag_lr: SAMN18797631). Metaproteomics data of the GDB sample is available at ProteomeXchange under accession PXD025505. The code used for the analysis is available at https://doi.org/10.6084/m9.figshare.14447553 and supplementary data of relevant results is available at https://doi.org/10.6084/m9.figshare.14447559.

Competing interests

The authors declare no competing interests.

Funding

SBB was supported by the Synergia grant (CRSII5_180241) through the Swiss National Science Foundation (in collaboration with Dr. Tom Battin at EPFL, Switzerland). PW acknowledges the European Research Council (ERC-CoG 863664). LdN, PW, and PM were supported by the Luxembourg National Research Fund (FNR; PRIDE17/11823097). BJK was supported by the FNR (C19/BM/13684739 and PRIDE17/11823097). VG was supported by “Probiotics in external applications (PBGL)”. CCL and MC were supported by the FNR (C17/SR/11687962).

Authors' contributions

SBB, VG, and CCL designed the study. SBB and RH performed the biomolecular extractions, while RH performed the metagenomic and metatranscriptomic sequencing. VG, SBB, LdN and CCL analysed the data. BJK performed the metaproteomic analyses. PM, MC and PW provided critical feedback and insights. All authors contributed to the writing and revision of the manuscript.

209 # Acknowledgements

210 We are thankful for the assistance of Audrey Frachet Bour, Lea Grandmougin, Janine Habier and
211 Laura Lebrun (LCSB) for laboratory support. The experiments presented in this paper were
212 carried out using the HPC facilities of the University of Luxembourg (https://hpc.uni.lu [19]).
213

Supplementary Information: Methods

Sample origin & collection

Human fecal samples were freshly collected from a healthy volunteer (GDB) and immediately flash-frozen in liquid nitrogen. The samples were stored at −80 °C until they were processed for biomolecular extraction.

Biomolecular extraction

To obtain high-molecular weight (HMW) DNA, we followed the protocol proposed recently [8], with minor modifications. Frozen stool sample was weighed out in triplicates, to 0.7g and aliquoted into phase-lock gel tubes (Fisher Scientific, Waltham, MA), along with a 4mm stainless steel grinding ball (RETSCH 22.455.0003). The sample was subsequently suspended in 500µL PBS (Fisher Scientific, Waltham, MA) with brief gentle vortexing at 10 second intervals repeated 5 times. Thereafter, 5uL of lytic enzyme solution (Qiagen, Hilden, Germany) was added and the samples were mixed by gentle inversion six times, then incubated for one hour at 37˚C. 12µL 20% (w/v) SDS (Fisher Scientific, Waltham, MA) was added followed by 500µL phenol:chloroform:isoamyl alcohol at pH 8 (Fisher Scientific, Waltham, MA). The samples were gently vortexed for five seconds, then centrifuged at 10,000g for five minutes. The aqueous phase was decanted into a new 2mL tube. Next, the DNA was precipitated with 90µL 3M sodium acetate (Fisher Scientific) and 500uL isopropanol (Fisher Scientific). After slowly inverting three times, samples were incubated at room temperature for 10 minutes, followed by centrifugation for 10 minutes at 10,000g. The supernatant was removed, and the pellet was washed twice with freshly prepared 80% (v/v) ethanol (Fisher Scientific). Washing was done by adding 1 ml of 80% EtOH, followed by centrifugation for 10 minutes at 10,000g. The pellet was then air dried with heating for ten minutes at 37˚C or until the pellet was matte in appearance, and then resuspended in 100µL nuclease-free water (Ambion, ThermoFisher Scientific, Waltham, MA). To the pellet, 1mL Qiagen buffer G2, 4µL Qiagen RNase A at 100mg/mL, and 25µL Qiagen Proteinase K were added. The samples were then gently inverted three times and incubated for 90 minutes at 56˚C. After the first 30 minutes, pellets were dislodged by a single gentle inversion. During the 90-minutes incubation, one Qiagen Genomic-tip 20/G column per triplicate sample was equilibrated with 1mL Qiagen buffer QBT and allowed to empty by gravity flow. Samples were gently inverted twice, applied to columns and allowed to flow through. Three stool extractions (triplicates for each

sample) were combined per column. Columns were then washed with 3mL Qiagen buffer QC, where 1 ml of QC buffer was added each time and allowed to drain the column. Next, the column was placed in a new, sterile 1.5 mL Eppendorf tube and the DNA was then eluted with 1mL of Qiagen buffer QF prewarmed to 56˚C. The eluted DNA was then precipitated by addition of 700µL isopropanol and incubated at room temperature for 10 minutes, followed by inversion and centrifugation for 15 minutes at 10,000g. The supernatant was carefully removed by pipette, and pellets were washed with 1mL 80% (v/v) ethanol. (Washing = add 1 ml EtOH, centrifuge for 10 minutes at 10,000g). Residual ethanol was removed by air drying ten minutes at 37˚C, followed by resuspension of the pellet in 100µL water overnight at 4˚C without agitation of any kind. The pooled sample was quantified using the Qubit Broad-Range DNA concentration kit, and was estimated at 323.35 ng/µL with an $OD_{260/280}$ = 1.85. The extracted HMW DNA was used for both short- and long-read sequencing. RNA was extracted from an aliquot of the same fecal sample using PowerMicrobiome RNA isolation kit (cat. no. 26000-50, MoBio) as suggested by the manufacturer. For the protein extractions, a modified protocol based on previously established sequential extraction method [20] was used. Briefly, proteins were precipitated by adding one volume of APP Buffer to the flow-through from an independent RNA purification, followed by mixing and incubation for 10 minutes at room temperature. After incubation, the mixture was centrifuged for 10 minutes at 12000 g and the pellet was washed twice in 70% ethanol, with 1 minute centrifuge cycles at 12000 g, and dried at room temperature for 7 minutes after removing excess ethanol. The pellet was then dissolved in 100µL ALO buffer and incubated for 5 minutes at 95 °C. After complete dissolution and denaturation of the protein, the sample was cooled to room temperature and centrifuged for 1 minute at 12000 g, from which the supernatant was collected for downstream protein analysis.

Sequencing

Short-read sequencing: All DNA samples were subjected to random shotgun sequencing. The sequencing libraries were prepared using Kapa hyperplus Kit (cat. no. 07962401001, Roche) for the fecal sample using the protocol provided with the kit. Enzymatic fragmentation time was 15 minutes to aim for 350bp average size. There was no additional PCR amplification of prepared libraries.

RNA samples for metaT analysis were subjected to rRNA depletion using the QIAseq FastSelect 5S/16S/23S kit (cat. no. 335921, Qiagen) for the fecal sample. Library preparation of rRNA-depleted RNA was done using TruSeq Stranded mRNA library preparation kit (cat. no.

20020594, Illumina) according to the protocol provided by the manufacturer with the exception of omitting the initial steps for mRNA pull down.

Both metaG and metaT libraries were quantified using Qubit HS assay (Invitrogen) and their quality was assessed on a Bioanalyzer HS chip (Agilent). We used the NextSeq500 (Illumina) instrument to perform the sequencing using 2x150bp read length at the LCSB Sequencing Platform.

Long-read sequencing: DNA library for the fecal sample was size selected using AMpure beads for longer fragments. The DNA was sheared using a G-tube (cat. no. 520079, Covaris) aiming for 8kb average size according to the protocol provided by the manufacturer. Library preparation for long read sequencing was done using genomic DNA ligation kit (SQK-LSK109) according to the protocol provided. Once all the library loaded on the flowcell was finished, the library was reloaded after either flowcell wash or nuclease flush. In total, the library was loaded 4 times to achieve 16Gbp of sequencing data for this fecal sample.

Data analysis

Snakemake (v. 5.18.1) [21] was used to implement the analysis workflow. We provide a brief description of the most important steps in the following.

Sequence data preprocessing

Short-reads: The raw short reads were trimmed and preprocessed with fastp (v. 0.20.0) [22] with a minimum length of 40 bp. FastQC (v. 0.11.9) [23] reports were generated from the processed FASTQ files. MetaT short reads from the GDB sample were filtered by discarding reads mapping to rRNA gene references included in the repository of SortMeRNA [24] (v4.2.0-10-g1358b9b, https://github.com/biocore/sortmerna) using BBDuk from the BBMap toolkit (v.38.86, kmer length set to 31 bp) [25]. Additionally, for the GDB sample, reads mapping to the human genome (GCF_000001405.38_GRCh38.p12) were removed using BBDuk (kmer length set to 31 bp, input and output quality encoding offset set to 33).

Long reads: For each sample except NWC, single-FAST5 files were converted to multi-FAST5 files using single_to_multi_fast5 from ont-fast5-api (v. 3.1.5), the resulting files were basecalled using guppy on a GPU node (v. 3.6.0+98ff765, configuration file dna_r9.4.1_450bps_modbases_dam-dcm-cpg_hac.cfg, disabled transmission of telemetry pings, chunk size of 1000, 8000 records per FASTQ file) and concatenated into a single FASTQ file. For NWC, no FAST5 were available and, thus, only the provided FASTQ file was used for the analysis.

Nanostat (v. 1.1.2) [26] reports were created from the FASTQ files using default parameters. As for the short reads, long reads of the GDB sample were filtered to remove reads mapping to the human genome (GCF_000001405.38_GRCh38.p12) using the same parameters.

Metagenomic assembly

Short-reads: Short-read assemblies were done using preprocessed reads, and MEGAHIT and metaSPAdes. MEGAHIT (v. 1.2.9) [27] was run using default parameters; metaSPAdes (v. 3.14.1) [28] was run using kmer lengths 21, 33, 55 and 77 bp.

Long-reads: Long-read assemblies were done using Flye and Raven. Flye (v. 2.8.1) [29] was run by providing the (processed) long reads in a FASTQ file (input parameter "--nano-raw") and with the flag "--meta". Raven (v. 1.2.2) [30] was run with default parameters. Assemblies were polished using long and short reads: one round of Racon (v. 1.4.13) [31] with long reads using the flag "--include-unpolished" where reads were mapped to contigs using BWA MEM (v. 0.7.17) [32] with the option "-x ont2d" and processed using samtools (v. 1.9); four rounds of Racon with short reads using the flag "--include-unpolished" where reads were mapped to contigs using BWA MEM and processed using samtools; one round of Medaka (v. 0.8.1) [33] with long reads using the model "r941_min_high".

Hybrid: Hybrid assemblies, i.e. using short and long reads together, were done using metaSPAdes and OPERA-MS. SPAdes was run with the flag "--meta" and the same k-mer lengths as the SR assemblies by additionally providing the long reads using the input parameter flag "--nanopore". OPERA-MS (v. v0.8.2-63-gc18b4f3) [15] was run using paired short reads, long reads and the SR assemblies created by MEGAHIT and metaSPAdes, respectively, using minimap2 [34] as the long read mapper. The assemblies were polished by running five rounds of Racon with short reads as described for the LR assemblies. If not stated otherwise, only polished contigs were used for the LR and HY assemblies in the following analysis steps.

Mapping rate and assembly coverage

For the mapping rate, the used reads were mapped back to the contigs and processed using BWA MEM and samtools in the same fashion as described above when polishing the LR and HY assemblies using Racon. For hybrid assemblies, both long and short reads were mapped to the polished contigs and the BAM files were merged using samtools. For the sample GDB, metatranscriptomic (metaT) short reads were also separately mapped to the (polished) contigs. Mapping statistics were computed from the BAM files using samtools' options "flagstat", to

determine the number of reads mapping back to the assemblies, and “idxstats” for per-contig mapping information. For GDB, metaT per-base coverage was computed for each assembly from the BAM files using bedtools (v. 2.29.2)[35] (utility “genomecov” with the parameter “-d”).

Assembly annotation

For each sample and assembly, protein prediction was done using Prodigal (v. 2.6.3) [36] using the option “-p meta”; the keyword “partial” in the headers of the obtained protein FASTA files was used to distinguish complete and partial proteins. Known antibiotic resistance factors were searched in the predicted proteins (after discarding the stop codon symbol “*” from the FASTA files) by running RGI (v. 5.1.1) [37] together with the CARD database (v. 3.1.0) [18] and DIAMOND (v. 0.8.36) [38] for protein alignments. Loose hits flagged as “nudged” by the tool were highlighted as such (i.e. as “nudged”) in the downstream analysis.

The tool barrnap (v. 0.9) [39] was run to predict rRNA genes on assembly contigs using the four provided databases of bacterial, archaeal, metazoan mitochondrial and eukaryotic rRNA genes, respectively. Predictions containing the word “partial” in their product annotation in the obtained GFF files were considered as partial hits.

Analysis

Assembly statistics were computed by running metaQUAST (v. 5.0.2) [40] without using any genome references, setting the minimum contig length to 0 bps and retrieving the statistics for the contig length thresholds of 0, 1000, 2000 and 5000 bps subsequently. Per sample, assemblies were compared using Mash (v. 2.2.2) [41]: sketches were computed per assembly using a k-mer length of 31 bps and a sketch size of 100000, and pairwise distances were then estimated. Per sample, proteins from all assemblies were clustered using MMseqs2 (v. 12.113e3) [42]. First, a database was created from a concatenated FASTA file of protein sequences (“--dbtype 1”). Then, option “linclust” with default parameters was used to perform the clustering and the obtained files were converted to tables using option “createtsv“. DIAMOND (v. 0.9.25) [38][43] with the option “blastp” and default parameters was used to align the predicted proteins against the UniProtKB/TrEMBL database (downloaded and created on August 24 2019 from http://ftp.uniprot.org/pub/databases/uniprot/current_release/knowledgebase/complete/, archive uniprot_trembl.fasta.gz) [44]. The created DAA files were converted to tables using option “view” and the parameter “--max-target-seqs 1”. When processing the hits, these were sorted per query and e-value in an ascending order and only the first hit was used. For GDB and metaT, using the

per-base coverage information computed for each assembly, average coverage was computed for the corresponding gene sequences of each predicted protein.

MS/MS acquisition and metaproteomic analysis

1µg of extracted proteins was denatured and briefly loaded on a SDS gel to produce one gel band. The reduction, alkylation and tryptic digestion of the proteins into peptides were performed in-gel. The tryptic peptides were extracted from the gel and desalted prior to mass spectrometry analysis. Peptides were analyzed using a nanoLC-MS/MS system (120 minutes gradient) connected to a Q-Exactive HF orbitrap mass spectrometer (Thermo Scientific, Germany) equipped with a nano-electrospray ion source. The Q-Exactive mass spectrometer was operated in data-dependent mode and the 10 most intense peptide precursor ions were selected for fragmentation and MS/MS acquisition.

For each assembly separately and for all assemblies together, the FASTA file of predicted proteins was concatenated with a cRAP database of contaminants [45] and with the human UniProtKB Reference Proteome prior metaproteomic search. In addition, reversed sequences of all protein entries were concatenated to the databases for the estimation of false discovery rates. The search was performed using SearchGUI-3.3.20 [46] with the X!Tandem [47], MS-GF+ [48] and Comet [49] search engines and the following parameters: Trypsin was used as the digestion enzyme, and a maximum of two missed cleavages was allowed. The tolerance levels for matching to the database was 10 ppm for MS1 and 0.2 Da for MS2. Carbamidomethylation of cysteine residues was set as a fixed modification and protein N-terminal acetylation and oxidation of methionines was allowed as variable modification. Peptides with length between 7 and 60 amino acids, and with a charge state composed between +2 and +4 were considered for identification. The results from SearchGUI were merged using PeptideShaker-1.16.45 [50] and all identifications were filtered in order to achieve a protein false discovery rate (FDR) of 1%.

Plots

Figures were generated in R (v. 4.0.2, https://www.r-project.org/) using, *inter alia*, Pheatmap (v. 1.0.12, https://github.com/raivokolde/pheatmap) for heatmap plots, UpSetR (v. 1.4.0) [51] for intersection plots, ggplot2 (v 3.3.2) [52] and its various extensions for other plot types, color palettes from the viridis (v. 0.5.1, developed by Stéfan van der Walt and Nathaniel Smith, https://github.com/sjmgarnier/viridis) and ggsci (v. 2.9, https://github.com/road2stat/ggsci)

399 packages and the patchwork package (v. 1.1.1, https://github.com/thomasp85/patchwork) for
400 combining plots.

401 References

402 1. Burgess DJ. Genomics: Next regeneration sequencing for reference genomes. Nat. Rev.
403 Genet. 2018. p. 125.

404 2. Amarasinghe SL, Su S, Dong X, Zappia L, Ritchie ME, Gouil Q. Opportunities and challenges
405 in long-read sequencing data analysis. Genome Biol. 2020;21:30.

406 3. Nicholls SM, Quick JC, Tang S, Loman NJ. Ultra-deep, long-read nanopore sequencing of
407 mock microbial community standards. Gigascience [Internet]. 2019;8. Available from:
408 http://dx.doi.org/10.1093/gigascience/giz043

409 4. Pollard MO, Gurdasani D, Mentzer AJ, Porter T, Sandhu MS. Long reads: their purpose and
410 place. Hum Mol Genet. 2018;27:R234–41.

411 5. Jain M, Koren S, Miga KH, Quick J, Rand AC, Sasani TA, et al. Nanopore sequencing and
412 assembly of a human genome with ultra-long reads. Nat Biotechnol. 2018;36:338–45.

413 6. Goldstein S, Beka L, Graf J, Klassen JL. Evaluation of strategies for the assembly of diverse
414 bacterial genomes using MinION long-read sequencing. BMC Genomics. 2019;20:23.

415 7. Logsdon GA, Vollger MR, Eichler EE. Long-read human genome sequencing and its
416 applications. Nat Rev Genet. 2020;21:597–614.

417 8. Moss EL, Maghini DG, Bhatt AS. Complete, closed bacterial genomes from microbiomes
418 using nanopore sequencing. Nat Biotechnol. 2020;38:701–7.

419 9. Nicholls SM, Aubrey W, De Grave K, Schietgat L, Creevey CJ, Clare A. On the complexity of
420 haplotyping a microbial community. Bioinformatics [Internet]. 2020; Available from:
421 http://dx.doi.org/10.1093/bioinformatics/btaa977

422 10. Stewart RD, Auffret MD, Warr A, Walker AW, Roehe R, Watson M. Compendium of 4,941
423 rumen metagenome-assembled genomes for rumen microbiome biology and enzyme discovery.
424 Nat Biotechnol. 2019;37:953–61.

425 11. Zhang H, Jain C, Aluru S. A comprehensive evaluation of long read error correction
426 methods. BMC Genomics. 2020;21:889.

427 12. Ryan R. Wick KEH. Benchmarking of long-read assemblers for prokaryote whole genome
428 sequencing. F1000Res [Internet]. Faculty of 1000 Ltd; 2019 [cited 2021 Mar 19];8. Available
429 from: https://www.ncbi.nlm.nih.gov/pmc/articles/PMC6966772/

430 13. Dohm JC, Peters P, Stralis-Pavese N, Himmelbauer H. Benchmarking of long-read
431 correction methods. NAR Genom Bioinform. 2020;2:lqaa037.

432 14. Watson M, Warr A. Errors in long-read assemblies can critically affect protein prediction.

433 Nat. Biotechnol. 2019. p. 124–6.

434 15. Bertrand D, Shaw J, Kalathiyappan M, Ng AHQ, Kumar MS, Li C, et al. Hybrid metagenomic
435 assembly enables high-resolution analysis of resistance determinants and mobile elements in
436 human microbiomes. Nat Biotechnol. 2019;37:937–44.

437 16. Haghshenas E, Asghari H, Stoye J, Chauve C, Hach F. HASLR: Fast Hybrid Assembly of
438 Long Reads. iScience. 2020;23:101389.

439 17. Somerville V, Lutz S, Schmid M, Frei D, Moser A, Irmler S, et al. Long-read based de novo
440 assembly of low-complexity metagenome samples results in finished genomes and reveals
441 insights into strain diversity and an active phage system. BMC Microbiol. 2019;19:143.

442 18. Alcock BP, Raphenya AR, Lau TTY, Tsang KK, Bouchard M, Edalatmand A, et al. CARD
443 2020: antibiotic resistome surveillance with the comprehensive antibiotic resistance database.
444 Nucleic Acids Res. 2020;48:D517–25.

445 19. Management of an academic HPC cluster: The UL experience [Internet]. [cited 2021 Mar
446 24]. Available from: https://ieeexplore.ieee.org/document/6903792

447 20. Roume H, Heintz-Buschart A, Muller EEL, Wilmes P. Sequential isolation of metabolites,
448 RNA, DNA, and proteins from the same unique sample. Methods Enzymol. 2013;531:219–36.

449 21. Köster J, Rahmann S. Snakemake—a scalable bioinformatics workflow engine.
450 Bioinformatics. 2012;28:2520–2.

451 22. Chen S, Zhou Y, Chen Y, Gu J. fastp: an ultra-fast all-in-one FASTQ preprocessor.
452 Bioinformatics. 2018;34:i884–90.

453 23. Andrews S, Others. FastQC: a quality control tool for high throughput sequence data.
454 Babraham Bioinformatics, Babraham Institute, Cambridge, United Kingdom; 2010.

455 24. Kopylova E, Noé L, Touzet H. SortMeRNA: fast and accurate filtering of ribosomal RNAs in
456 metatranscriptomic data. Bioinformatics. 2012;28:3211–7.

457 25. Bushnell B. BBMap: A fast, accurate, splice-aware aligner [Internet]. Lawrence Berkeley
458 National Lab. (LBNL), Berkeley, CA (United States); 2014 Mar. Report No.: LBNL-7065E.
459 Available from: https://www.osti.gov/biblio/1241166

460 26. De Coster W, D'Hert S, Schultz DT, Cruts M, Van Broeckhoven C. NanoPack: visualizing
461 and processing long-read sequencing data. Bioinformatics. 2018;34:2666–9.

462 27. Li D, Liu C-M, Luo R, Sadakane K, Lam T-W. MEGAHIT: an ultra-fast single-node solution
463 for large and complex metagenomics assembly via succinct de Bruijn graph. Bioinformatics.
464 2015;31:1674–6.

465 28. Nurk S, Meleshko D, Korobeynikov A, Pevzner PA. metaSPAdes: a new versatile
466 metagenomic assembler. Genome Res. 05 2017;27:824–34.

467 29. Kolmogorov M, Bickhart DM, Behsaz B, Gurevich A, Rayko M, Shin SB, et al. metaFlye:
468 scalable long-read metagenome assembly using repeat graphs. Nat Methods. 2020;17:1103–
469 10.

30. Vaser R, Šikić M. Raven: a de novo genome assembler for long reads [Internet]. Cold Spring Harbor Laboratory. 2020 [cited 2021 Mar 19]. p. 2020.08.07.242461. Available from: https://www.biorxiv.org/content/10.1101/2020.08.07.242461v1

31. Vaser R, Sović I, Nagarajan N, Šikić M. Fast and accurate de novo genome assembly from long uncorrected reads. Genome Res. 2017;27:737–46.

32. Li H. Aligning sequence reads, clone sequences and assembly contigs with BWA-MEM [Internet]. arXiv [q-bio.GN]. 2013. Available from: http://arxiv.org/abs/1303.3997

33. medaka [Internet]. Github; [cited 2021 Mar 19]. Available from: https://github.com/nanoporetech/medaka

34. Li H. Minimap2: pairwise alignment for nucleotide sequences. Bioinformatics. 2018;34:3094–100.

35. Quinlan AR, Hall IM. BEDTools: a flexible suite of utilities for comparing genomic features. Bioinformatics. 2010;26:841–2.

36. Hyatt D, Chen G-L, LoCascio PF, Land ML, Larimer FW, Hauser LJ. Prodigal: prokaryotic gene recognition and translation initiation site identification. BMC Bioinformatics. 2010;11:119.

37. Jia B, Raphenya AR, Alcock B, Waglechner N, Guo P, Tsang KK, et al. CARD 2017: expansion and model-centric curation of the comprehensive antibiotic resistance database. Nucleic Acids Res. 2017;45:D566–73.

38. Buchfink B, Xie C, Huson DH. Fast and sensitive protein alignment using DIAMOND. Nat Methods. 2015;12:59–60.

39. Seemann T. barrnap 0.9: rapid ribosomal RNA prediction. Google Scholar. 2013;

40. Mikheenko A, Saveliev V, Gurevich A. MetaQUAST: evaluation of metagenome assemblies. Bioinformatics. 2016;32:1088–90.

41. Ondov BD, Treangen TJ, Melsted P, Mallonee AB, Bergman NH, Koren S, et al. Mash: fast genome and metagenome distance estimation using MinHash. Genome Biol. 2016;17:132.

42. Steinegger M, Söding J. MMseqs2 enables sensitive protein sequence searching for the analysis of massive data sets. Nat Biotechnol. 2017;35:1026–8.

43. biomickwatson. A simple test for uncorrected insertions and deletions (indels) in bacterial genomes [Internet]. 2018 [cited 2021 Mar 19]. Available from: http://www.opiniomics.org/a-simple-test-for-uncorrected-insertions-and-deletions-indels-in-bacterial-genomes/

44. The Universal Protein Resource (UniProt). Nucleic Acids Res. 2008-1;36:D190–5.

45. cRAP protein sequences [Internet]. [cited 2021 Mar 19]. Available from: https://www.thegpm.org/crap/

46. Barsnes H, Vaudel M. SearchGUI: A Highly Adaptable Common Interface for Proteomics Search and de Novo Engines. J Proteome Res. 2018;17:2552–5.

47. Langella O, Valot B, Balliau T, Blein-Nicolas M, Bonhomme L, Zivy M. X!TandemPipeline: A

506 Tool to Manage Sequence Redundancy for Protein Inference and Phosphosite Identification. J
507 Proteome Res. 2017;16:494–503.

508 48. Kim S, Pevzner PA. MS-GF+ makes progress towards a universal database search tool for
509 proteomics. Nat Commun. 2014;5:5277.

510 49. Eng JK, Jahan TA, Hoopmann MR. Comet: an open-source MS/MS sequence database
511 search tool. Proteomics. 2013;13:22–4.

512 50. Vaudel M, Burkhart JM, Zahedi RP, Oveland E, Berven FS, Sickmann A, et al.
513 PeptideShaker enables reanalysis of MS-derived proteomics data sets. Nat Biotechnol.
514 2015;33:22–4.

515 51. Conway JR, Lex A, Gehlenborg N. UpSetR: an R package for the visualization of
516 intersecting sets and their properties. Bioinformatics. Oxford Academic; 2017;33:2938–40.

517 52. Wickham H. ggplot2: Elegant Graphics for Data Analysis. Springer; 2016.

518

Figures and Tables

Figures

Fig. 1: **Discrepancy and uniqueness of predicted proteins in assemblies. i** Number of proteins (total and partial) predicted by Prodigal in each assembly and sample. The color corresponds to the tool used for metagenomic assembly. **ii** Number of shared assembly proteins which were clustered using MMSesq2 per sample. Each protein cluster was labeled by the combination of assembly tools represented by the clustered proteins (i.e., the assembly where these proteins originated from). The depicted number of shared proteins per assembly tool combination is the total protein count over all associated clusters. Top 20 combinations are shown. The number of proteins found in clusters representing all assembly tools is highlighted in red; the number of proteins exclusive to an assembly is highlighted in orange.

i)

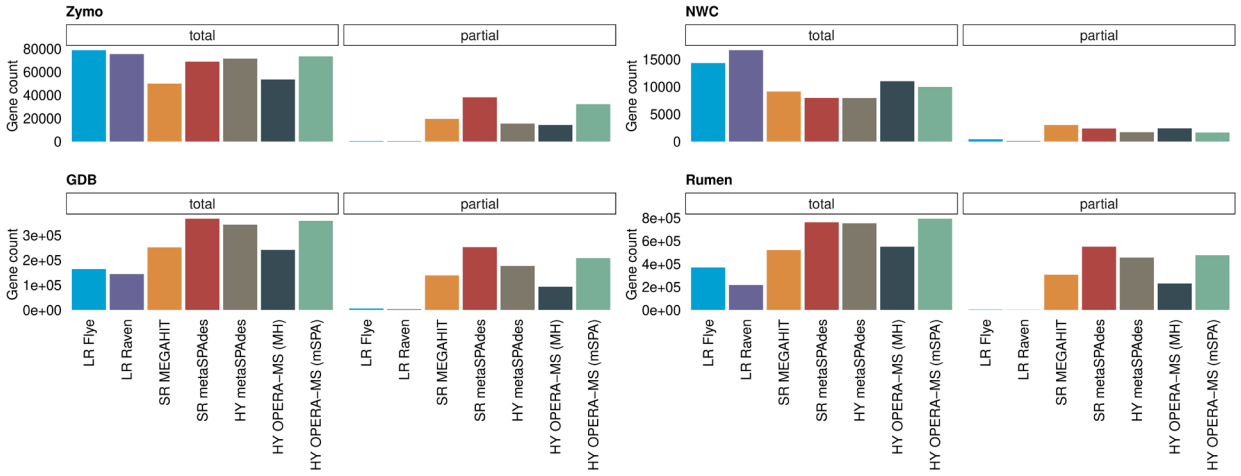

ii)

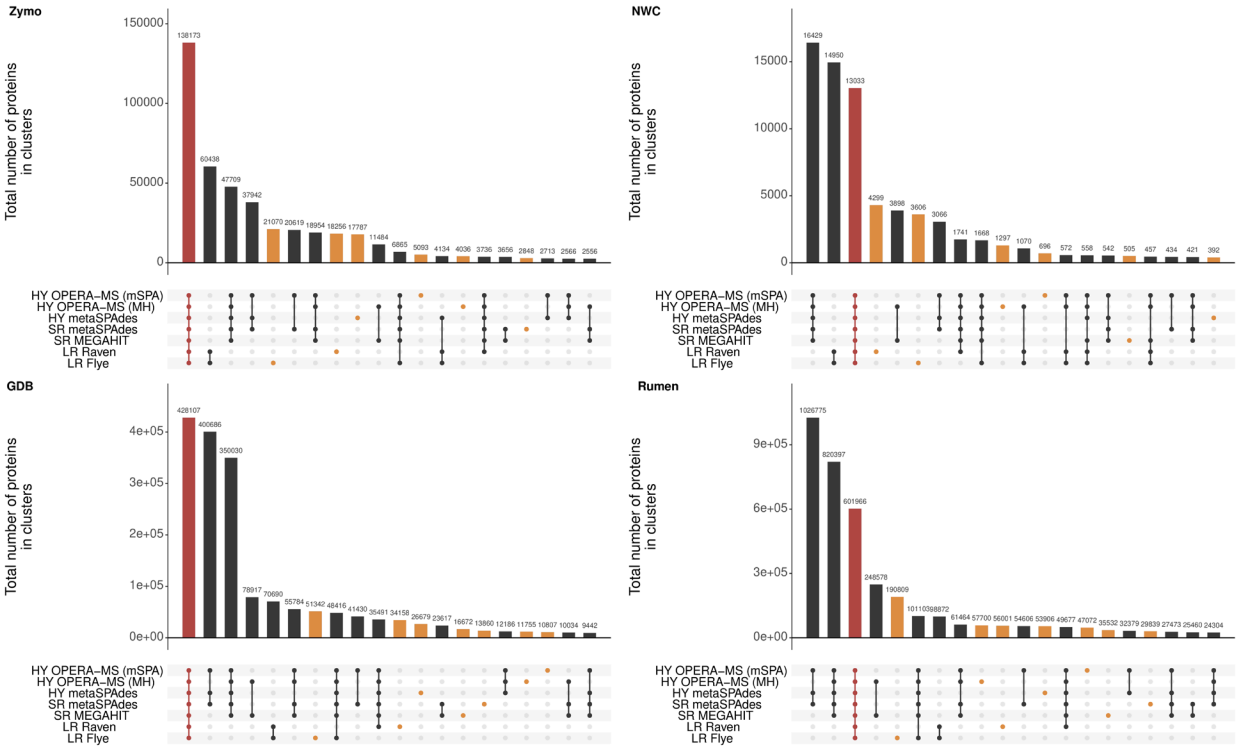

Fig. 2: **Assembly affects antimicrobial resistance gene identification**. **i** Number of hits (total, "strict" and "nudged") for each assembly and sample when searching the assembly proteins in the CARD database using RGI. Sample NWC was excluded because no hits were found in any of its assemblies. "Nudged" hits are loose hits flagged as "nudged" by RGI; the remaining hits are "strict" hits. **ii** Number of AROs which were covered by "strict" RGI hits by different assemblies per sample. The bar plot shows the number of shared AROs per assembly tools combination. **iii** Metatranscriptomic (metaT) coverage of the two coding sequences (CDSs) from the long-read (LR) assembly constructed with Flye and having a "nudged" RGI hit to ARO 3004454 (a chloramphenicol acetyltransferase) in sample GDB. The x-axis represents the contig coordinates and the y-axis the metaT coverage. The amino acid sequence of the two CDSs and the ARO is included in the plot.

i)

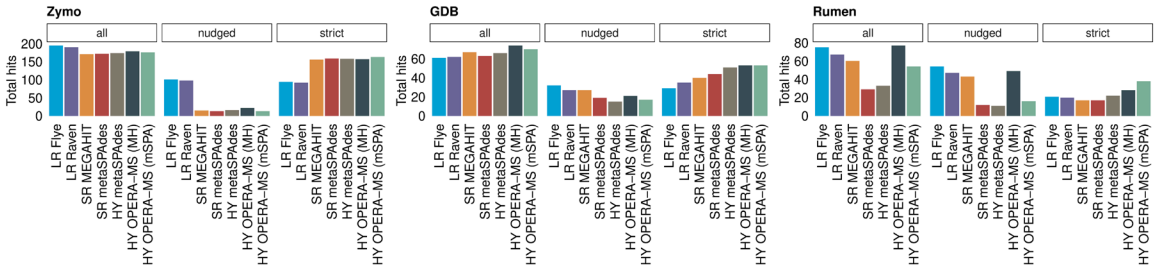

ii)

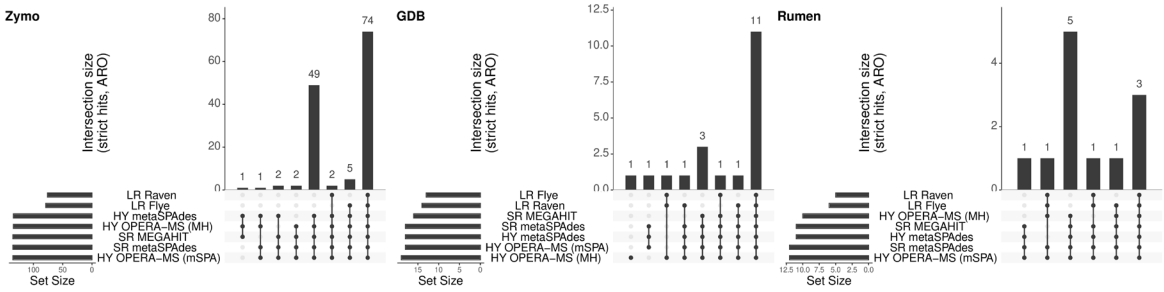

iii)

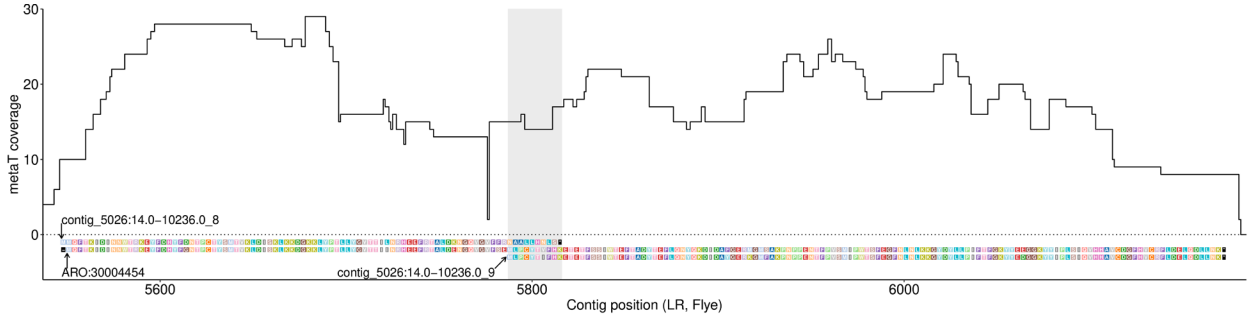

Supplementary figures

Supp. Fig. 1: **Assembly statistics**. Assembly statistics for each assembly and sample including the total number of contigs, number of N bases per 100kbp, L50 value (number of contigs), N50 value (in bps), the length of the largest contig (in bps), and the total assembly length (in bps). The color corresponds to the tool used for metagenomic assembly.

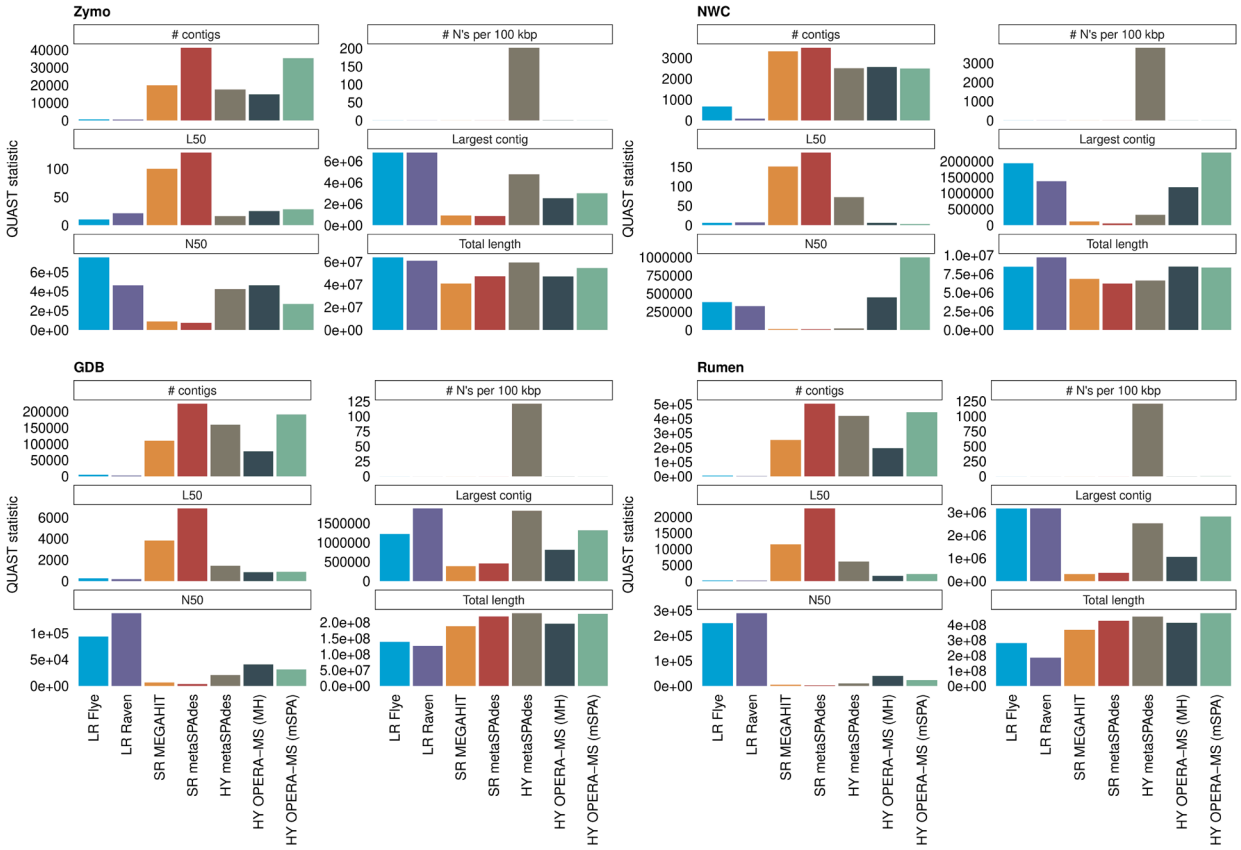

Supp. Fig. 2: **Mapping rate of metagenomic reads**. Mapping rate of metagenomic reads to each assembly for each sample considering all contigs and contigs being at least 1000, 2000 and 5000bps long. The color corresponds to the tool used for metagenomic assembly.

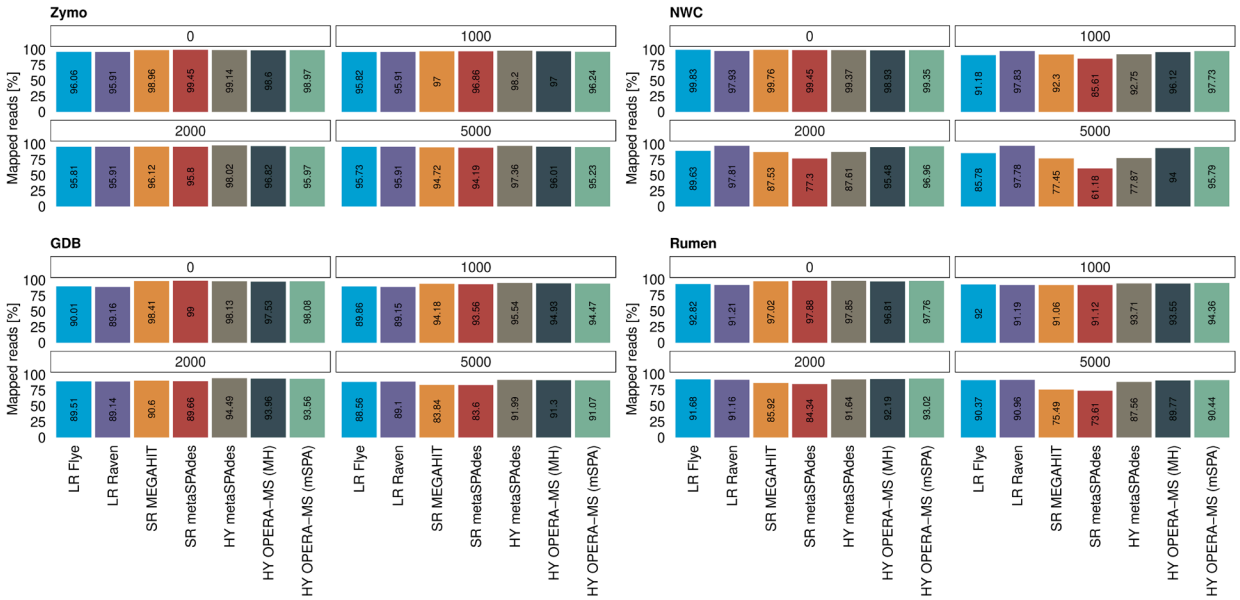

Supp. Fig. 3: **Mapping rate of metatranscriptomic reads**. Mapping rate of metatranscriptomic reads to each assembly in GDB considering all contigs and contigs being at least 1000, 2000 and 5000bps long. The color corresponds to the tool used for metagenomic assembly.

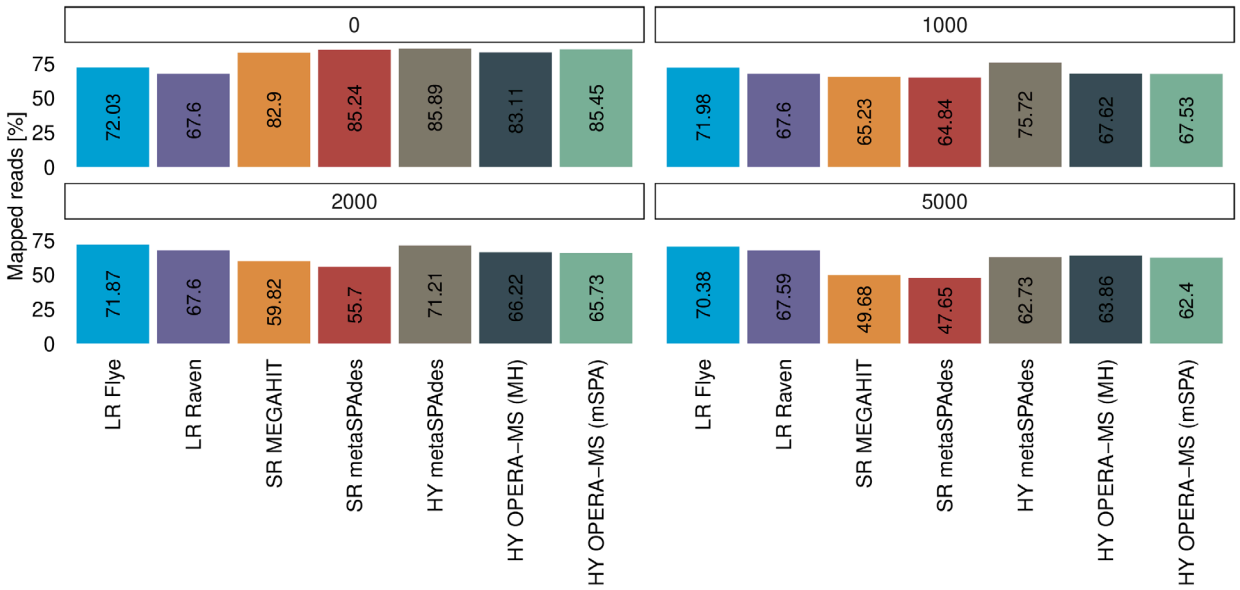

570 **Supp. Fig. 4**: **Assembly similarity**. Heatmap of assembly dissimilarity of each sample. The cell
571 color corresponds to the estimated dissimilarity value and the rounded value is shown in each
572 cell: higher values (yellow) indicate higher dissimilarity, lower values (dark purple) indicate high
573 similarity. Assemblies were grouped using hierarchical clustering (linkage method “complete”):
574 the resulting trees are shown in the heatmaps.

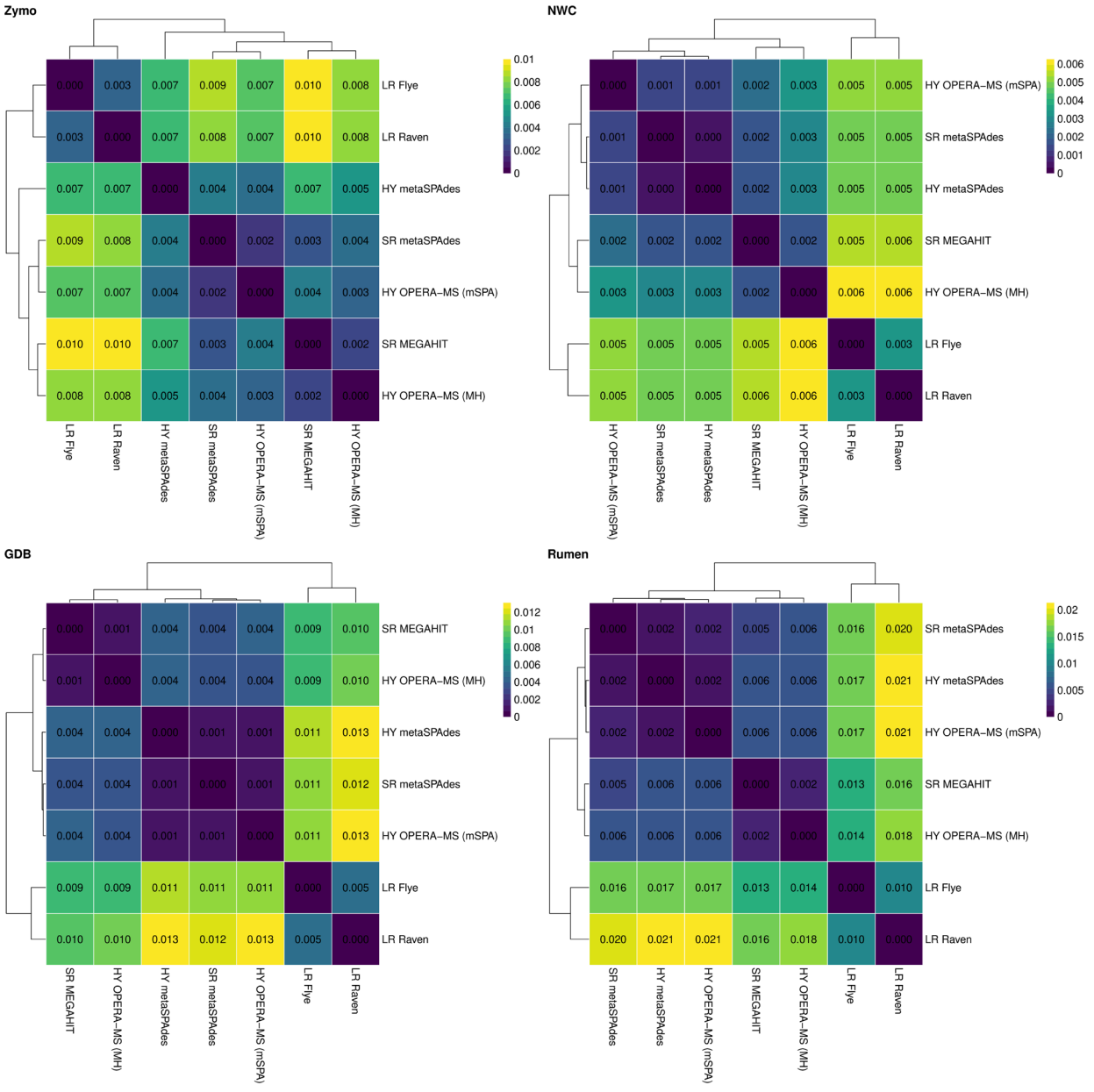

575
576

Supp. Fig. 5: **Protein sequence search in the UniProtKB/TrEMBL nr database**. Density distribution of the query/subject length ratios of the best hit obtained in the protein sequence search in the UniProtKB/TrEMBL nr database for each assembly and sample. The color corresponds to the tool used for metagenomic assembly.

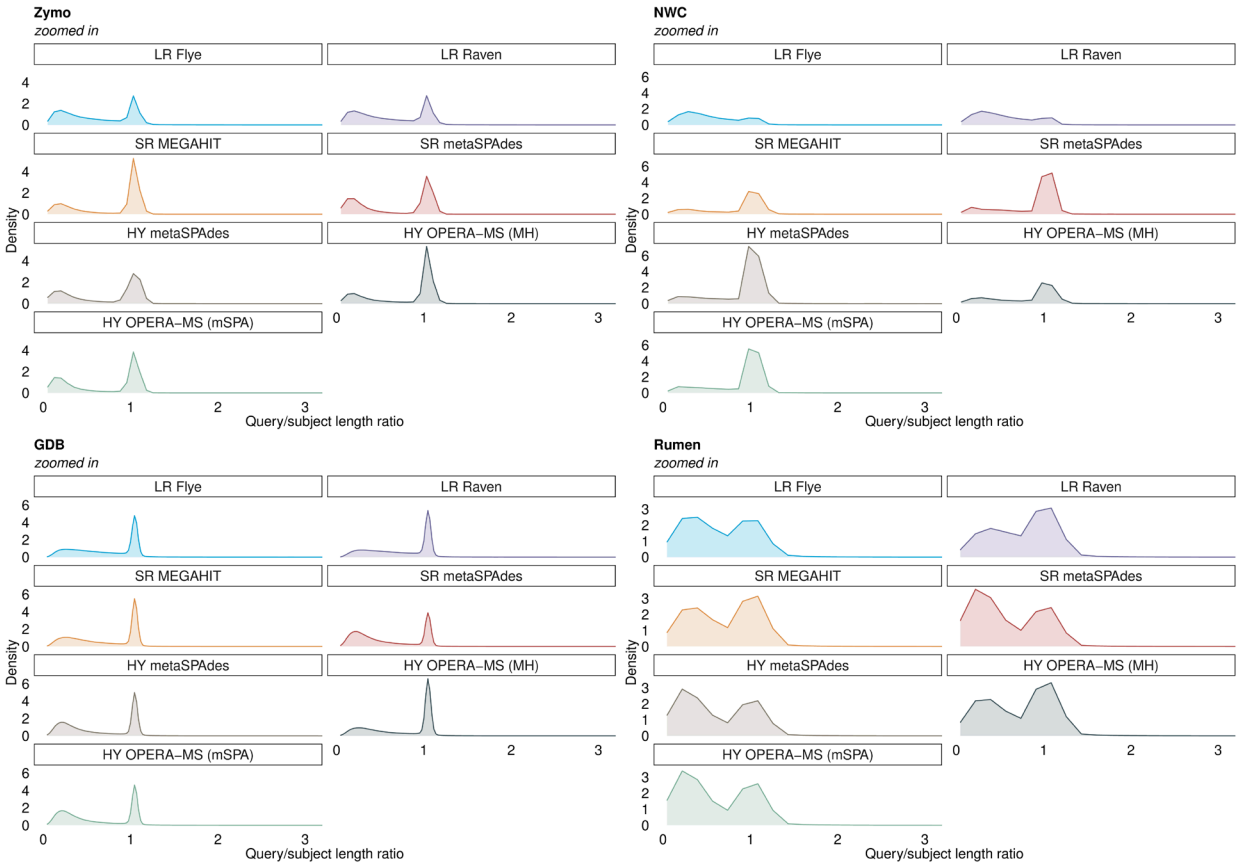

583 **Supp. Fig. 6**: **Prediction of rRNA genes**. Number of rRNA genes (complete, partial and total)
584 found by barrnap in assembly contigs using different rRNA gene databases (Archaea, Bacteria,
585 Eukaryota and Metazoan mitochondria) for each assembly and sample. The color corresponds to
586 the tool used for metagenomic assembly.

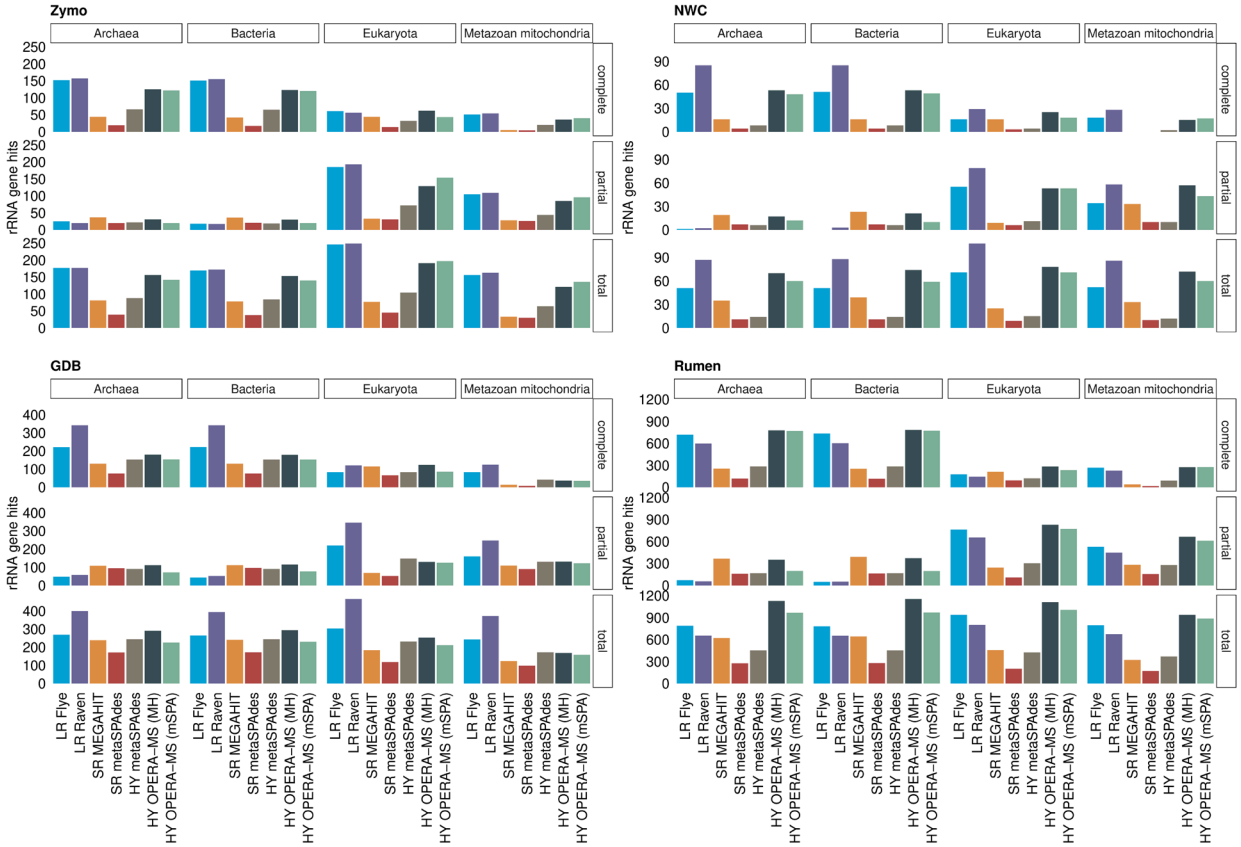

587

588

Supplementary tables

Supp. Tab. 1: **Proteins assigned to exclusive AROs in GDB**. Information on proteins from GDB assemblies assigned to AROs found exclusively in SR and HY assemblies when considering only "strict" RGI hits, i.e., AROs 3000194, 3002999 and 3004454. The table includes the protein ID, the RGI hit information (RGI Detection Paradigm, ARO term of top hit in CARD, percent identity of match to top hit in CARD, ARO ID, CARD detection model type, ARO's drug class and mechanism, flag whether the hit was "nudged" from "loose" to "strict"), the assembly tool, additional protein information (contig ID, protein number on the source contig, start and end coordinates on the contig, Prodigal's annotation information) and average metaT coverage.

ORF_ID	Cut_Off	Best_Hit_ARO	Best_Identities	ARO	Model_type	Drug.Class	Resistance.Mechanism	Nudged	tool	contig_id	prot_num	start	end	strand	info	ave_cov
k141_88921_2	Perfect	tetW	100	3000194	protein homolog model	tetracycline antibiotic	antibiotic target protection		SR MEGAHIT	k141_88921	2	808	2727	-1	ID=5257_2;partial=00;start_type=ATG;rbs_motif=GGAGG;rbs_spacer=5-10bp;gc_cont=0.531	14.81666667
k141_44684_172	Perfect	CblA-1	100	3002999	protein homolog model	cephalosporin	antibiotic inactivation		SR MEGAHIT	k141_44684	172	210664	211554	-1	ID=6454_172;partial=00;start_type=ATG;rbs_motif=TAAA;rbs_spacer=12bp;gc_cont=0.485	18.57687991
k141_37405_1	Strict	Campylobacter coli chloramphenicol acetyltransferase	96.14	3004454	protein homolog model	phenicol antibiotic	antibiotic inactivation		SR MEGAHIT	k141_37405	1	46	669	-1	ID=42126_1;partial=00;start_type=ATG;rbs_motif=GGAGG;rbs_spacer=5-10bp;gc_cont=0.370	18.33974359
k141_59580_1	Strict	tetW	100	3000194	protein homolog model	tetracycline antibiotic	antibiotic target protection	True	SR MEGAHIT	k141_59580	1	1	1071	-1	ID=46787_1;partial=10;start_type=ATG;rbs_motif=AGGAGG;rbs_spacer=5-10bp;gc_cont=0.430	5.194211018
k141_105836_1	Strict	tetW	97.83	3000194	protein homolog model	tetracycline antibiotic	antibiotic target protection	True	SR MEGAHIT	k141_105836	1	500	640	1	ID=67436_1;partial=01;start_type=ATG;rbs_motif=GGAGG;rbs_spacer=5-10bp;gc_cont=0.511	0
NODE_12_length_289084_cov_116.206895_175	Perfect	CblA-1	100	3002999	protein homolog model	cephalosporin	antibiotic inactivation		SR metaSPAdes	NODE_12_length_289084_cov_116.206895	175	215250	216140	-1	ID=12_175;partial=00;start_type=ATG;rbs_motif=TAAA;rbs_spacer=12bp;gc_cont=0.485	18.57687991
NODE_3961_length_5598_cov_17.248325_7	Strict	Campylobacter coli chloramphenicol acetyltransferase	96.02	3004454	protein homolog model	phenicol antibiotic	antibiotic inactivation		SR metaSPAdes	NODE_3961_length_5598_cov_17.248325	7	4994	5596	1	ID=3961_7;partial=01;start_type=ATG;rbs_motif=GGAGG;rbs_spacer=5-10bp;gc_cont=0.371	17.85406302
NODE_8958_length_2718_cov_51.879591_1	Perfect	tetW	100	3000194	protein homolog model	tetracycline antibiotic	antibiotic target protection		SR metaSPAdes	NODE_8958_length_2718_cov_51.879591	1	352	2271	1	ID=8958_1;partial=00;start_type=ATG;rbs_motif=GGAGG;rbs_spacer=5-10bp;gc_cont=0.531	14.76770833
contig_210:1.0-492442.0_427	Strict	CblA-1	100	3002999	protein homolog model	cephalosporin	antibiotic inactivation	True	LR Flye	contig_210:1.0-492442.0	427	345531	346178	1	ID=1098_427;partial=00;start_type=ATG;rbs_motif=TAAA;rbs_spacer=12bp;gc_cont=0.475	21.51388889
contig_210:1.0-492442.0_428	Strict	CblA-1	100	3002999	protein homolog model	cephalosporin	antibiotic inactivation	True	LR Flye	contig_210:1.0-492442.0	428	346165	346422	1	ID=1098_428;partial=00;start_type=ATG;rbs_motif=None;rbs_spacer=None;gc_cont=0.504	10.89147287
contig_2107:1.0-6493.0_10	Strict	tetW	100	3000194	protein homolog model	tetracycline antibiotic	antibiotic target protection	True	LR Flye	contig_2107:1.0-6493.0	10	6589	6672	-1	ID=1107_10;partial=01;start_type=Edge;rbs_motif=None;rbs_spacer=None;gc_cont=0.488	1.94047619
contig_5026:14.0-10236.0_8	Strict	Campylobacter coli chloramphenicol acetyltransferase	96.1	3004454	protein homolog model	phenicol antibiotic	antibiotic inactivation	True	LR Flye	contig_5026:14.0-10236.0	8	5547	5816	1	ID=4198_8;partial=00;start_type=ATG;rbs_motif=GGAGG;rbs_spacer=3-4bp;gc_cont=0.356	19.90740741
contig_5026:14.0-10236.0_9	Strict	Campylobacter coli chloramphenicol acetyltransferase	96.09	3004454	protein homolog model	phenicol antibiotic	antibiotic inactivation	True	LR Flye	contig_5026:14.0-10236.0	9	5788	6174	1	ID=4198_9;partial=00;start_type=ATG;rbs_motif=3Base/5BMM;rbs_spacer=13-15bp;gc_cont=0.377	16.88113695
contig_720:1.0-180574.0_143	Strict	tetW	100	3000194	protein homolog model	tetracycline antibiotic	antibiotic target protection	True	LR Flye	contig_720:1.0-180574.0	143	113111	113386	1	ID=4795_143;partial=00;start_type=ATG;rbs_motif=AGGAGG;rbs_spacer=5-10bp;gc_cont=0.504	2.347826087
contig_720:1.0-180574.0_145	Strict	tetW	99.58	3000194	protein homolog model	tetracycline antibiotic	antibiotic target protection	True	LR Flye	contig_720:1.0-180574.0	145	114312	115028	1	ID=4795_145;partial=00;start_type=TTG;rbs_motif=AGGAG/GGAGG;rbs_spacer=11-12bp;gc_cont=0.531	6.154811715
Utg192512:1.0-55330.0_65	Strict	tetW	100	3000194	protein homolog model	tetracycline antibiotic	antibiotic target protection	True	LR Raven	Utg192512:1.0-55330.0	65	53663	53938	1	ID=184_65;partial=00;start_type=ATG;rbs_motif=GGAGG;rbs_spacer=5-10bp;gc_cont=0.507	0.753623188
Utg192512:1.0-55330.0_66	Strict	tetW	99.38	3000194	protein homolog model	tetracycline antibiotic	antibiotic target protection	True	LR Raven	Utg192512:1.0-55330.0	66	53926	54432	1	ID=184_66;partial=00;start_type=TTG;rbs_motif=AGGAG/GGAGG;rbs_spacer=11-12bp;gc_cont=0.525	2.362919132
Utg193156:1.0-36767.0_53	Strict	tetW	95.28	3000194	protein homolog model	tetracycline antibiotic	antibiotic target protection	True	LR Raven	Utg193156:1.0-36767.0	53	36661	37176	-1	ID=450_53;partial=00;start_type=ATG;rbs_motif=None;rbs_spacer=None;gc_cont=0.535	0.426356589
Utg193258:12.0-497832.0_131	Strict	CblA-1	100	3002999	protein homolog model	cephalosporin	antibiotic inactivation	True	LR Raven	Utg193258:12.0-497832.0	131	112535	113116	-1	ID=489_131;partial=00;start_type=ATG;rbs_motif=TAAA;rbs_spacer=12bp;gc_cont=0.479	22.70618557
Utg194422:1.0-41914.0_3	Strict	tetW	97.96	3000194	protein homolog model	tetracycline antibiotic	antibiotic target protection	True	LR Raven	Utg194422:1.0-41914.0	3	2784	3251	1	ID=908_3;partial=00;start_type=TTG;rbs_motif=AGGAG/GGAGG;rbs_spacer=11-12bp;gc_cont=0.528	1.386752137
Utg196264:1.0-22987.0_38	Strict	tetW	95.74	3000194	protein homolog model	tetracycline antibiotic	antibiotic target protection	True	LR Raven	Utg196264:1.0-22987.0	38	22691	23314	1	ID=1406_38;partial=00;start_type=GTG;rbs_motif=None;rbs_spacer=None;gc_cont=0.535	4.284461538
Utg197488:1.0-10247.0_3	Strict	tetW	100	3000194	protein homolog model	tetracycline antibiotic	antibiotic target protection	True	LR Raven	Utg197488:1.0-10247.0	3	1339	1545	-1	ID=1693_3;partial=00;start_type=ATG;rbs_motif=GGAGG;rbs_spacer=5-10bp;gc_cont=0.522	3.579710145
NODE_1_length_1822148_cov_145.496205_549	Perfect	CblA-1	100	3002999	protein homolog model	cephalosporin	antibiotic inactivation		HY metaSPAdes	NODE_1_length_1822148_cov_145.496205	549	611846	612736	-1	ID=1_549;partial=00;start_type=ATG;rbs_motif=TAAA;rbs_spacer=12bp;gc_cont=0.485	18.57687991
NODE_230_length_104252_cov_9.790458_35	Perfect	tetW	100	3000194	protein homolog model	tetracycline antibiotic	antibiotic target protection		HY metaSPAdes	NODE_230_length_104252_cov_9.790458	35	38586	40505	1	ID=230_35;partial=00;start_type=ATG;rbs_motif=GGAGG;rbs_spacer=5-10bp;gc_cont=0.531	7.6453125
NODE_348_length_69013_cov_11.179239_18	Perfect	tetW	100	3000194	protein homolog model	tetracycline antibiotic	antibiotic target protection		HY metaSPAdes	NODE_348_length_69013_cov_11.179239	18	10767	12686	1	ID=348_18;partial=00;start_type=ATG;rbs_motif=GGAGG;rbs_spacer=5-10bp;gc_cont=0.531	7.191145833
NODE_5177_length_5598_cov_17.248325_7	Strict	Campylobacter coli chloramphenicol acetyltransferase	96.02	3004454	protein homolog model	phenicol antibiotic	antibiotic inactivation		HY metaSPAdes	NODE_5177_length_5598_cov_17.248325	7	4994	5596	1	ID=5177_7;partial=01;start_type=ATG;rbs_motif=GGAGG;rbs_spacer=5-10bp;gc_cont=0.371	17.85406302
opera_contig_1206_6	Perfect	tetW	100	3000194	protein homolog model	tetracycline antibiotic	antibiotic target protection		HY OPERA-MS (MH)	opera_contig_1206	6	3769	5688	1	ID=1206_6;partial=00;start_type=ATG;rbs_motif=GGAGG;rbs_spacer=5-10bp;gc_cont=0.531	14.81666667
opera_contig_1626_1	Strict	Campylobacter coli chloramphenicol acetyltransferase	96.14	3004454	protein homolog model	phenicol antibiotic	antibiotic inactivation		HY OPERA-MS (MH)	opera_contig_1626	1	46	669	-1	ID=1626_1;partial=00;start_type=ATG;rbs_motif=GGAGG;rbs_spacer=5-10bp;gc_cont=0.370	18.33974359
opera_contig_17222_1	Strict	tetW	97.83	3000194	protein homolog model	tetracycline antibiotic	antibiotic target protection	True	HY OPERA-MS (MH)	opera_contig_17222	1	500	640	1	ID=17222_1;partial=01;start_type=ATG;rbs_motif=GGAGG;rbs_spacer=5-10bp;gc_cont=0.511	0
opera_contig_76911_177	Perfect	CblA-1	100	3002999	protein homolog model	cephalosporin	antibiotic inactivation		HY OPERA-MS (MH)	opera_contig_76911	177	215801	216691	-1	ID=76911_177;partial=00;start_type=ATG;rbs_motif=TAAA;rbs_spacer=12bp;gc_cont=0.485	18.57687991
opera_contig_1579_7	Strict	Campylobacter coli chloramphenicol acetyltransferase	96.02	3004454	protein homolog model	phenicol antibiotic	antibiotic inactivation		HY OPERA-MS (mSPA)	opera_contig_1579	7	4994	5596	1	ID=1579_7;partial=01;start_type=ATG;rbs_motif=GGAGG;rbs_spacer=5-10bp;gc_cont=0.371	17.85406302
opera_contig_2773_1	Perfect	tetW	100	3000194	protein homolog model	tetracycline antibiotic	antibiotic target protection		HY OPERA-MS (mSPA)	opera_contig_2773	1	352	2271	1	ID=2773_1;partial=00;start_type=ATG;rbs_motif=GGAGG;rbs_spacer=5-10bp;gc_cont=0.531	14.76770833
opera_contig_190552_176	Perfect	CblA-1	100	3002999	protein homolog model	cephalosporin	antibiotic inactivation		HY OPERA-MS (mSPA)	opera_contig_190552	176	215253	216143	-1	ID=190552_176;partial=00;start_type=ATG;rbs_motif=TAAA;rbs_spacer=12bp;gc_cont=0.485	18.57687991